Bioresource Technology 408 (2024) 131190

Contents lists available at ScienceDirect

Bioresource Technology

journal homepage: www.elsevier.com/locate/biortech

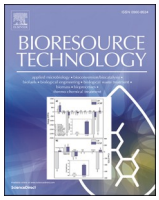

Bio-based production of *cis,cis*-muconic acid as platform for a sustainable polymers production

Filippo Molinari [a], Andrea Salini [b], Aniello Vittore [a], Orlando Santoro [a], Lorella Izzo [a], Salvatore Fusco [b], Loredano Pollegioni [a], Elena Rosini [a,*]

[a] Department of Biotechnology and Life Sciences, University of Insubria, via J. H. Dunant 3, 21100 Varese, Italy
[b] Biochemistry and Industrial Biotechnology (BIB) Laboratory, Department of Biotechnology, University of Verona, Strada le Grazie 15, 37134 Verona, Italy

HIGHLIGHTS

- ccMA was selectively produced from engineered *E. coli* in bioreactor.
- High productivity was obtained in optimized pulse-feeding fermentation.
- The growing cells approach shows lower E-factor and PMI parameters vs. resting cells.
- A fully bioderived polymer with tailored physico-chemical properties was produced.

GRAPHICAL ABSTRACT

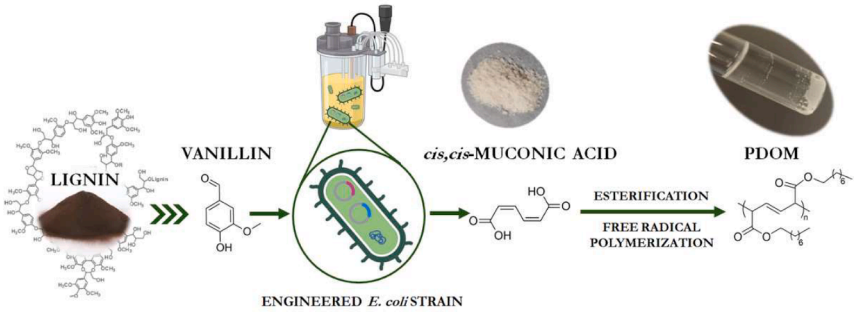

ARTICLE INFO

Keywords:
Biotransformation
Renewable biomasses
Vanillin
System biocatalysis
Bio-based polymers
Lignin valorization

ABSTRACT

Production of the high industrial value *cis,cis*-muconic acid (ccMA) from renewable biomasses is of main interest especially when biological (green) processes are used. We recently generated a *E. coli* strain expressing five recombinant enzymes to convert vanillin (VA, from lignin) into ccMA. Here, we optimized a growing cell approach in bioreactor for the ccMA production. The medium composition, fermentation conditions, and VA addition were tuned: pulse-feeding VA at 1 mmol/h allowed to reach 5.2 g/L of ccMA in 48 h (0.86 g ccMA/g VA), with a productivity 4-fold higher compared to the resting cells approach, thus resulting in significantly lower E-factor and Process Mass Intensity green metric parameters. The recovered ccMA has been used as building block to produce a fully bioderived polymer with rubber-like properties. The sustainable optimized bioprocess can be considered an integrated approach to develop a platform for bio-based polymers production from renewable feedstocks.

1. Introduction

Muconic acid (2,4-hexadienedioic acid) is a six-carbon di-unsaturated dicarboxylic acid which occurs in three isomeric forms: *cis, cis*- (ccMA), *trans,trans*-, and *cis,trans*-muconic acid. ccMA can be produced by chemical synthesis (from non-renewable oil-derived

* Corresponding author at: Department of Biotechnology and Life Sciences, University of Insubria, Varese, Italy.
E-mail address: elena.rosini@uninsubria.it (E. Rosini).

https://doi.org/10.1016/j.biortech.2024.131190
Received 4 April 2024; Received in revised form 28 July 2024; Accepted 30 July 2024
Available online 31 July 2024

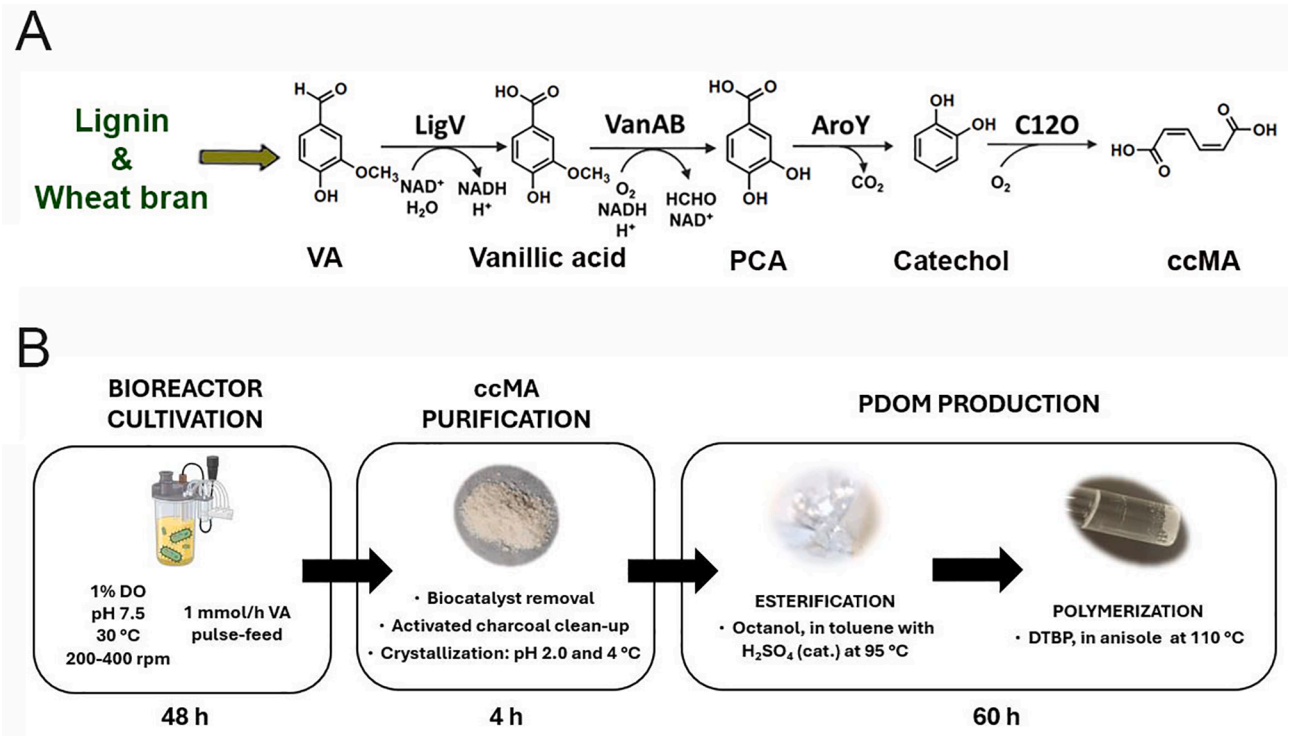

Fig. 1. A) Biosynthetic pathway to produce ccMA from VA catalyzed by an engineered *E. coli* strain expressing the multi-enzymatic system comprising the vanillin dehydrogenase LigV, the vanillic acid O-demethylase VanAB, the protocatechuate decarboxylase AroY, and the catechol 1,2-dioxygenase C12O. B) Flowchart of the established protocol for the PDOM production of ccMA recovered from the bioconversion of VA in a bioreactor cultivation system using growing cells.

chemicals), bioconversion of lignin (using lignin-based aromatic compounds), and microbial fermentation of sugars; for a recent review see (Choi et al., 2020). ccMA is a molecule with a recognized industrial value (the estimated global market in 2024 was of US$ 119.4 million) (https://www.researchandmarkets.com/reports/5562422/muconic-acid-market-global-industry-trends): it can be hydrogenated into adipic acid (AA), a widely applied building block for the production of nylons and polyurethanes, and can be used as the starting material to synthesize terephthalic acid (TPA) for the manufacturing of the plastic polymer polyethylene terephthalate (PET) (Zhang et al., 2015). Both AA and TPA are also used in cosmetic, pharmaceutical, textile and food sectors.

Notably, bacteria which produce ccMA from aromatics can use the ones present in lignin hydrolysates as substrates (Kohlstedt et al., 2018). Lignin can be treated to generate mixtures of aromatics through thermochemical (Long et al., 2014) and biological depolymerization (Pollegioni et al., 2015; Vignali et al., 2022). Lignin is strongly underutilized: 98 % is simply burned for energy supply. In the past, a number of efforts focused on improving both productivity and yield of high value-added compounds from lignin conversion via metabolic engineering of various bacteria. The current biological production of ccMA (and related compounds) primarily focuses on incorporating synthetic pathways into selected microorganisms to convert intermediate metabolites of the natural shikimate pathway into ccMA (Choi et al., 2020). ccMA bioconversion from fermentable substrates has been carried out at the laboratory and at the pilot scale: the most promising strategies depend on inhibiting ccMA degradation pathways (to promote its accumulation) and on overexpressing heterologous enzymes involved in converting lignin-derived aromatics. For a recent review, see Rosini et al., 2023. The highest ccMA productivity reported figures of 64.5 g/L in 120 h with an engineered *E. coli* strain (Choi et al., 2019) and 22.5 g/L in 118 h with an engineered *S. cerevisiae* strain (Wang et al., 2022). On the other hand, for the production of ccMA from lignin-derived aromatics, the use of engineered lignin-utilizing microorganisms such as *C. glutamicum*, *P. putida*, *Amicolatopsis* sp. and *R. opacus*, is generally preferred, due to their resistance to high concentrations of phenolic compounds and their innate ability to metabolize lignin-derived substrates (Becker and Wittmann, 2019; Choi et al., 2020; Rosini et al., 2023). Two of the most notable results are the production of 85 g/L of ccMA from catechol in 36 h using an engineered *C. glutamicum* strain (Becker et al., 2018) and of 55.4 g/L of ccMA from p-coumaric acid in 72 h using an engineered *P. putida* strain (Johnson et al., 2016).

Recently, our group set up a bioprocess to produce ccMA based on the optimization of the extraction procedures of ferulic acid (FA) from wheat bran (WB) and of vanillin (VA) from lignin, and the engineering of an *E. coli* strain expressing up to seven recombinant enzymes (Molinari et al., 2023). Starting from the multi-enzymatic cascade process set up to convert VA into ccMA (Vignali et al., 2021), we assembled this pathway in a single-engineered *E. coli* K-12 MG1655 RARE strain (Fig. 1A): compared to the cell-free bioconversion system, the commercial enzyme xanthine oxidase catalyzing the oxidation of VA into vanillic acid and the THF cofactor-dependent demethylase LigM catalyzing the demethylation of vanillic acid into protocatechuic acid (PCA) have been substituted by the dehydrogenase LigV and the demethylase VanAB. Next, the decarboxylase AroY, and the dioxygenase C12O converted lignin-derived VA into ccMA with a conversion yield above 95 % (4.2 mg of ccMA/g of Kraft lignin in 30 min).

In this study, we optimised ccMA production from VA, using the abovementioned engineered *E. coli* strain in a growing cells approach to allow better control of the reaction conditions and to obtain a final greater ccMA titer, by tuning medium composition, mixing, oxygen supply, and VA feeding. Noteworthy, the produced ccMA has been recovered, purified and used as building block for the production of a fully bioderived polymer, such as poly(dioctylmuconate) (PDOM), with tailored physico-chemical properties. The optimized integrated biological conversion of VA into ccMA holds great promise to set up a platform to produce polymers starting from renewable biomasses, towards a sustainable and biobased economy.

2. Materials and methods

2.1. Strain, growth medium and reagents

The *E. coli* MG1655 RARE strain (Kunjapur et al., 2014) carrying the plasmids pETDuet-1:AroY-C12O and pCDFDuet-1:VanAB-LigV was designed in a previous study (Molinari et al., 2023). Luria Bertani broth (Lennox), Terrific broth (modified), glycerol, D-(+)-glucose, α-lactose monohydrate, Antifoam 204, methanol (ACS Grade, ≥99 %), formic acid (ACS Grade, ≥98 %), sulfuric acid (ACS Reagent, 95–98 %), activated charcoal (DARCO®, 100 mesh particle size) and analytical grade standards of VA (4-hydroxy-3-methoxybenzaldehyde), vanillic acid (4-hydroxy-3-methoxybenzoic acid), protocatechuic acid (3,4-dihydroxybenzoic acid), catechol (1,2-dihydroxybenzene) and ccMA were purchased by Merck KGaA (Darmstadt, Germany).

2.2. Bioreactor cultivations: Growing cell approach

Cultivations were performed in 2.5 L bioreactor vessels (BioBook compact – Kbiotech, Switzerland), autoclaved at 121 °C for 20 min before usage. Inoculum cultures of the engineered strain were grown in 50 mL of LB containing appropriate antibiotics in 250 mL flasks at 30 °C and shaking at 180 rpm for 20 h. Culture aliquots (about 25 mL, equal to about 125 OD_{600nm}) were centrifuged at 4000 g, 4 °C for 10 min and the obtained bacterial pellets were resuspended using 20 mL of sterile medium collected from each bioreactor vessel. Cultivations were initiated by inoculating the cell suspension into the bioreactors through a sterile rubber septum at an initial $OD_{600nm} \approx 0.1$. Each batch cultivation was carried out in 1 L medium at 30 °C at a stirring of 200 rpm (Rushton impeller) for 24–48 h. The composition of the medium was: 50 g/L TB powder, 10 g/L glycerol, 0.5 g/L glucose, 2 g/L of lactose, 0.005 % (v/v) Antifoam 204 and appropriate antibiotics (unless otherwise stated). The cultivation conditions and the parameters controlled during the growth in bioreactor are reported in supplementary materials.

VA was added by pulse-feeding a 1 M solution in ethanol at a rate of 1 mL/h (unless otherwise stated). Specifically, the pump was active for 1 min at a flow rate of 1 mL/min to reach a concentration of about 1 mM of VA in the bioreactor at each feeding step. Different operational conditions have been tested (see supplementary materials). Samples were withdrawn at different times to evaluate the amount of biomass as well as the medium concentration of carbon sources, acetate, ethanol, metabolic intermediates, and the final product (i.e., ccMA). As general rule, for the optimization of fermentation medium, samples were withdrawn every hour for the first 8 h of cultivation in bioreactor as well as after 24 h (see section 3.1); to monitor the bioconversion into ccMA, samples were collected after starting the VA feeding, with a variable frequency (from 1 to 6 h timespan) (see section 3.2).

The procedure used for ccMA purification is reported in supplementary materials.

2.3. Bioconversion: Resting cell assay

The *E. coli* recombinant strain was grown in the bioreactor (see section 2.2), without the VA addition. Samples were withdrawn from the bioreactor at different growth phases. Cells were harvested by centrifugation (2500 g, 20 min, 4 °C), washed once in 200 mM Tris-HCl pH 8.0 and resuspended in the same buffer to have a final concentration of 350 mg cell wet weight (cww)/mL. The whole-cell biotransformation reactions were carried out in 1 mL final volume, into a 2 mL plastic tube. Biotransformations were carried out in 200 mM Tris-HCl pH 8.0 containing 70 mg_{cww}/mL of recombinant *E. coli* cells and 10 mM of VA. All reactions were performed at 37 °C on a rotatory shaker. The biocatalytic process was monitored by withdrawing at different times 100 µL of the reaction mixture for HPLC analysis (see supplementary materials).

2.4. Growth analysis

The optical density of the bacterial culture was spectrophotometrically recorded at 600 nm using the MSE PRO Single Beam UV/VIS spectrophotometer: the experimental data points were analyzed by the Gompertz equation (Zwietering et al., 1990) to build growth curves and calculate the maximum specific growth rate (μmax) and the weight-optical density ratio (g/OD_{600}). Besides spectrophotometric analysis, 10 mL of the bacterial culture were filtered by dead-end filtration using a 0.22 µm PTFE filter (previously weighted). The filter was washed with MilliQ water and weighed to record the cww. Then, the filter was dried in an oven at 70 °C for 1 day and kept in a desiccator jar at room temperature for 1 day before being weighed to record the cells dry weight (cdw). The weight-optical density ratio was estimated by linear regression over the experimental points plotted as total optical density versus weight (either cww or cdw).

2.5. Synthetic procedures

All manipulations involving air-sensitive compounds were carried out under nitrogen atmosphere using standard Schlenk techniques. All chemicals were purchased from Merck or TCI and used as received, unless otherwise stated. Anisole and toluene were dried over $CaCl_2$ prior to use.

^{1}H- and ^{13}C-{1H} NMR spectra were recorded at 25 °C on a Bruker AV400 spectrometer operating at 400 and 100 MHz for ^{1}H and ^{13}C, respectively, in deuterochloroform. Spectra were calibrated against the residual portion impurity of the deuterated solvent. ATR-FTIR spectra were recorded on a Cary 630 FTIR spectrometry (Agilent Technologies) at room temperature with 16 scans and a resolution of 4 cm^{-1}. M_n and $Đ$ values were determined against polystyrene standards by GPC analyses performed on a Jasco apparatus equipped with a Shodex KF-804L column, operating at a flow rate of 1 mL/min, in THF, 30 °C.

Thermal characterization was performed by Stare system DSC 3 (Mettler Toledo, Milano, Italy) and by Stare system TGA 2 (Mettler Toledo). DSC samples were heated from 40 to 130 °C, cooled down to −90 °C and heated again to 130 °C at a rate of 10 °C/min, using a 50 mL/min nitrogen flow rate. The glass transition temperatures (T_g) were determined from the second heating ramp. The thermal degradation properties were investigated by heating the sample from 25 to 800 °C at a rate of 10 °C/min under nitrogen atmosphere.

Procedures for synthesis of *cis,cis*-dioctyl muconate and its radical polymerization are reported in supplementary materials.

3. Results and discussion

3.1. Optimization of medium formulation and growth analysis by the resting cell approach

The valorization of the lignin fraction is still challenging. In this view, an engineered *E. coli* strain harboring genes encoding four different recombinant enzymes (LigV, VanAB, AroY and C12O) was developed to convert VA into ccMA. This engineered strain, when utilized in a biocatalytic process using resting cells (70 g cww/L) converted 10 mM (1.42 g/L) VA into ccMA with a > 95 % yield in 2 h (Molinari et al., 2023). In the present work, the aforementioned engineered *E. coli* strain was used in a growing cells bioconversion strategy in a bioreactor. The medium composition was formulated to maintain operational conditions similar to the ones utilized for the whole-cell bioconversion system optimized in a previous study (Molinari et al., 2023): 50 g/L TB powder and 10 g/L (or 0.008 % v/v) glycerol were used. A novelty has been introduced for the expression of the overall pathway: to improve the economic sustainability of the whole process, the recombinant proteins expression was induced using lactose instead of isopropyl β-D-1-thiogalactopyranoside (IPTG), which is cheaper and not toxic for *E. coli* cells (Dvorak et al., 2015). Lactose concentration has been

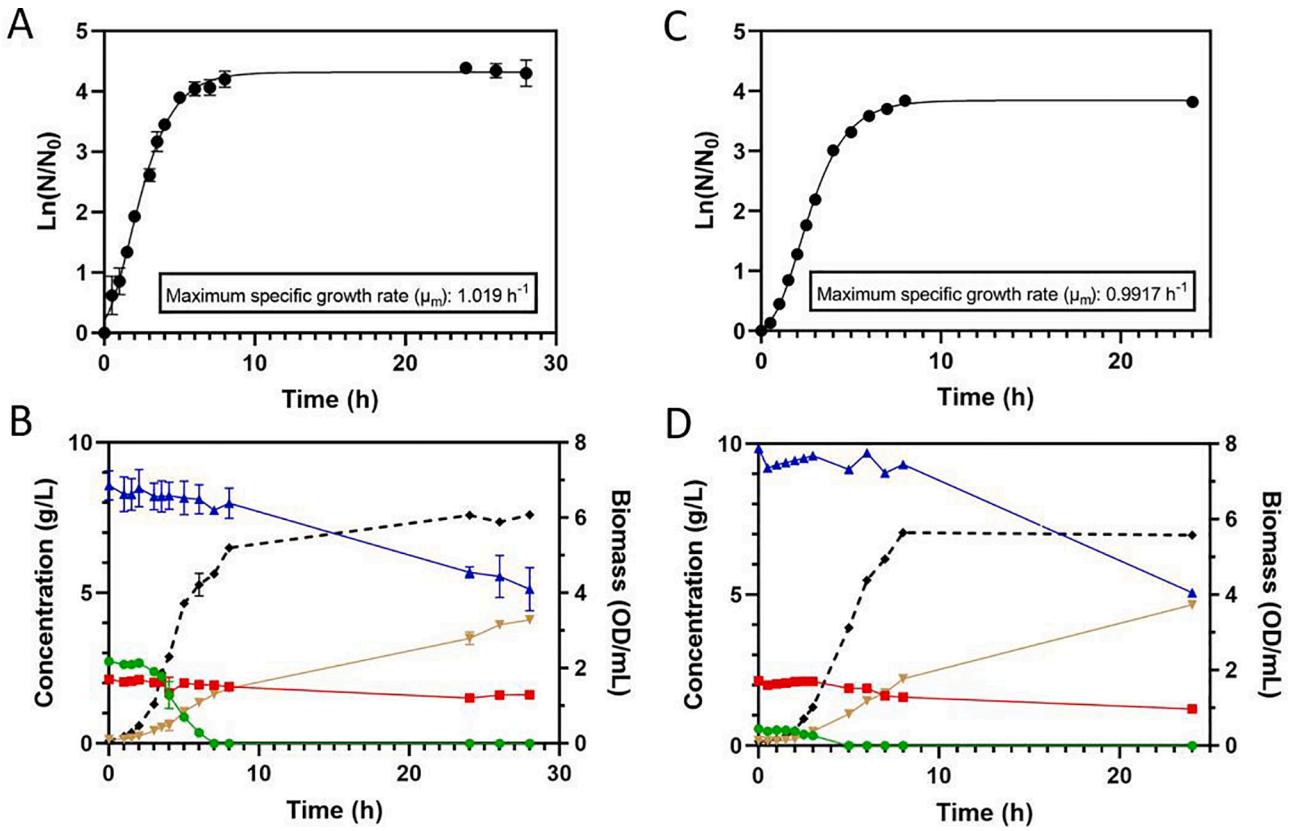

Fig. 2. Growth curve, metabolic profile and biomass concentration of the engineered strain grown without the addition of VA. A,C) Growth curve of the engineered strain in presence of 2 g/L lactose, and 3 g/L (A) or 0.5 g/L (C) glucose and calculated using the modified Gompertz equation (Zwietering et al., 1990). Data were collected from two independent biological replicates. B,D) Metabolic profile (continuous line) and biomass concentration (black, dotted line) of the engineered strain of panels A and C, respectively. (B): glucose (green) is completely consumed after 7 h while ≈80 % lactose (red; ≈1.6 g/L) remains in the medium after 28 h of growth. (D): glucose (green) is completely consumed after 5 h while ≈55 % lactose (red; ≈1.1 g/L) remains in the medium after 24 h fermentation. Glycerol and acetate labels are in blue and yellow, respectively.

adjusted to achieve high levels of expression of the different recombinant proteins (Blommel et al., 2007; Mayer et al., 2014; Studier, 2005). Since the expression of the pathway's recombinant enzymes was previously induced using 0.5 mM IPTG (Molinari et al., 2023), 2 g/L lactose was added to the fermentation medium to achieve a similar level of expression, as reported in (Gaglione et al., 2019). Noteworthy, an additional advantage of using lactose as the inducer is that glucose can be added to the fermentation medium to prevent lactose uptake and metabolism, while allowing rapid growth of the recombinant strain to the desired biomass level before protein induction starts, in the so-called "auto-inducing medium" expression (Blommel et al., 2007). Hence, lactose and glucose have been added to the growth medium to make it auto-inducing. The amount of glucose needed to generate a new *E. coli* cell during growth under aerobic conditions corresponds to $\approx 2.6 \times 10^9$ molecules, a figure obtained by summing the molecules needed for carbon atoms ($\approx 2 \times 10^9$; BNID 101859) and for energy during aerobic growth ($\approx 3\text{-}6 \times 10^8$; BNID 101778, 114702) (Phillips and Milo, 2009). Since the concentration of *E. coli* K-12 MG1655 cells at 1 OD/mL is $\approx 7 \times 10^8$ cell/mL (BNID 104831) (Sezonov et al., 2007), the amount of glucose needed for *E. coli* growth based on a certain generation number (G) was calculated according to Eq. (1):

$$Glucose\ consumption\left(\frac{g}{L}\right) = K\left(\frac{mg}{OD}\right) * N_i \left(\frac{OD}{mL}\right) * 2^G \quad (1)$$

where K (0.54 mg/OD) represents the amount of glucose utilized to produce $\approx 7 \times 10^8$ *E. coli* cells and N_i is the initial optical density of the culture. Since it is reported that starting lactose auto-induction during the log phase could inhibit bacterial growth resulting in low saturation density cultures (Cardoso et al., 2020), the culture should reach the late-log phase before starting the recombinant proteins expression. In order to reach a high amount of biomass before recombinant proteins induction starts, and based on Eq. (1), an *E. coli* culture with an initial OD/mL of 0.1 should grow up to 6.4 OD/mL (6th generation) using 3.45 g/L of glucose. Accordingly, 3 g/L of glucose was added to the medium.

The pH value of the growth medium was maintained at 7.5 by adding 3 M NaOH, thus allowing both the engineered strain to grow and the recombinant enzymes to work at their optimal pH value. Based on these assumptions, the final composition of the fermentation medium was: 50 g/L TB powder, 10 g/L glycerol, 3 g/L glucose, 2 g/L lactose, pH 7.5. Glycerol was kept in the medium since it can be used as a carbon source without causing the inhibition of lactose metabolism, hence allowing the expression of recombinant proteins. Lastly, in order to reach a compromise between the (high) conversion rate and the (rapid) growth of *E. coli* cells, the temperature was set at 30 °C.

The addition of VA to the fermentation medium prior to the inoculum could result in growth inhibition (Fitzgerald et al., 2004). In order to identify the optimal growth phase for VA addition, the bioconversion yields by the engineered strain *E. coli* MG1655 RARE pCDFDuet-1:LigV-VanAB pETDuet-1:AroY-C12O were assayed by harvesting cells from the bioreactor at different times during growth and setting up bioconversion reactions with resting cells, in a 1 mL final reaction volume. Moreover, the metabolic profile was analyzed to understand when carbon sources were depleted in the growth medium, with particular attention to glucose consumption. Cultivations in bioreactor were started by inoculating an amount of pre-inoculum culture to have an initial OD/mL of ≈0.1. In the aforementioned conditions, the engineered strain had a specific growth rate (μ) equal to 1.02 ± 0.04 h^{-1} (Fig. 2A) and a

Table 1
ccMA production yield obtained by bioconversion reactions of 10 mM VA using resting cells harvested from the cultivation using different media formulations.

Glucose (g/L)	Lactose (g/L)	Harvesting time (h)	ccMA production yield (%)
3	2	8	0.11
		24	5.4
0.5	2	6	32.0
		8	22.6
		24	27.6
0.5	4	6	9.8
		8	21.3

saturation density of 6.0 ± 0.2 OD/mL (Fig. 2B). HPLC analysis of the medium showed the complete consumption of glucose after 7 h of growth while lactose and glycerol remained at the concentration of 1.6 g/L and 5.1 g/L, respectively, up to 28 h of growth (Fig. 2B).

The ccMA production level of the engineered strain was assayed by bioconversions of VA using resting cells harvested at 8 h (i.e. one hour after glucose was completely consumed) and at 24 h of growth in bioreactor. Despite the complete conversion of VA into vanillic acid, only a small fraction of VA was converted into ccMA: ≈0.1 % and ≈5.4 % yield was achieved by the cells collected at 8 h and at 24 h of growth, respectively (Table 1). The inducer of the lactose operon is the metabolite allolactose, generated from the transglycosylation of lactose catalyzed by the enzyme β-galactosidase (Matthews, 2005). The fact that

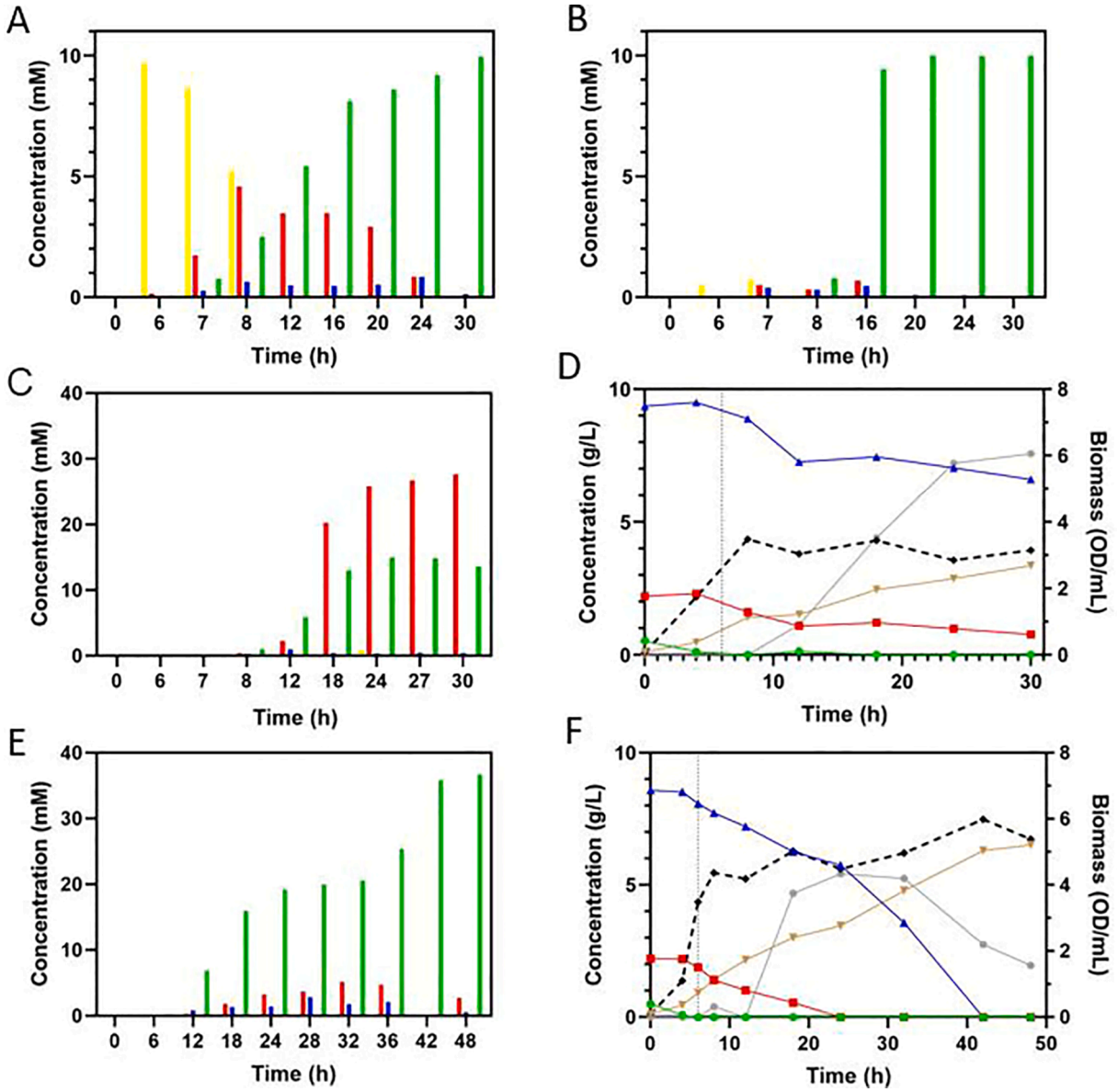

Fig. 3. Time course of the bioconversion of 10 mM VA added to growing cells using different strategies. A) Spike mode: 10 mmol of VA was added in the bioreactor 6 h after the growth started. B) Pulse-feed mode: 6 h after the growth started, 10 mmol of VA was added to the bioreactor through a 1 mmol/h pulse-feed that lasted for 10 h. The metabolites label are as follows: VA is yellow, vanillic acid is red, protocatechuic acid is blue, catechol is brown and ccMA is green. C,E) Time course of the bioconversion of 40 mM VA added through a 2 mmol/h (C) or 1 mmol/h (E) pulse-feed. The bioconversion labels are as follows: VA is yellow, vanillic acid is red, PCA is blue, catechol is brown and ccMA is green. D) Metabolic profile (continuous line) and biomass concentration (black, dotted line) of the bioconversion in panel C: glucose (green) is completely consumed after 4 h, ≈40 % lactose (red; ≈0.8 g/L) and ≈65 % glycerol (blue; ≈6.5 g/L) remained in the medium after 30 h of fermentation. F) Metabolic profile (continuous line) and biomass concentration (dotted line) of the bioconversion in panel E: glucose (green) is completely consumed after 4 h, lactose (red) after 24 h and glycerol (blue) after 42 h. The labels for acetate and ethanol are in yellow and grey, respectively. The vertical dotted line in panels D and E indicates when the VA pulse-feed started.

lactose was still present in the medium after 24 h (i.e. 1.6 g/L, Fig. 2B) points to a low expression of β-galactosidase under these growing conditions. This could be due to the persistence of glucose in the fermentation medium until the culture has already reached the initial stationary phase (Fig. 2B), causing a weak induction of the lactose operon.

To solve this drawback, the amount of glucose was decreased to allow the cells to start using lactose during the exponential phase. According to Eq. (1), the amount of glucose needed to reach the early exponential phase (≈1.0 OD/mL) is 0.5 g/L. In addition to using a lower concentration of glucose, the inducer concentration was evaluated at 2 or 4 g/L. At lower lactose level, the engineered strain showed a specific growth rate equal to 1.22 ± 0.08 h^{-1} (Fig. 2C) and a saturation density of 5.6 OD/mL (Fig. 2D). Glucose was completely consumed after 5 h of growth, while 1.1 g/L and 5.1 g/L of lactose and glycerol, respectively, were present up to 24 h of growth. As expected, *E. coli* starts metabolising lactose after glucose has been depleted, i.e. between the 3rd and 5th hour of growth (Fig. 2D). Under this condition, resting cells bioconversions were set up using cells harvested one hour after glucose was completely consumed (i.e. after 6 h of fermentation), as well as at 8 and 24 h. The highest conversion yield (≈32 %) was obtained with cells harvested at 6 h (Table 1), highlighting the ability of the engineered strain to convert VA into ccMA as early as 1 h after glucose is completely consumed. Since the increase in the amount of lactose could improve the pathway's enzymes expression and, therefore, the bioconversion yield, the engineered strain was grown in a medium with double the amount of lactose (4 g/L): however, this led to a decrease in the specific growth rate in bioreactor (0.795 h^{-1}, see supplementary materials). Moreover, the VA conversion yield for resting cells was only of 9.8 % after 6 h vs. 32 % achieved in the same timeframe by cells cultivated on 2 g/L of lactose (Table 1). These results point to a potential metabolic burden at the highest lactose concentration which, in turn, could result in a decreased yield of ccMA production.

Based on these evidences, the medium formulation containing 0.5 g/L glucose and 2 g/L lactose with VA addition after 6 h from the start of the culture growth was used in bioreactor cultivations and bioconversions (see Section 3.2 below). The presence of 0.005 % (v/v) Antifoam 204 did not alter the specific growth rate, metabolic profile and saturation density (see supplementary materials), so it was used for the following bioreactor cultivations.

3.2. Bioconversion optimization in bioreactor: A growing cell strategy

Since it has been reported that VanA activity is inhibited by a high amount of vanillic acid in the reaction system (Chen et al., 2021), it has been supposed that the feeding setup of VA could significantly affect the ccMA production. Thus, two different strategies of VA feeding were evaluated: i) single spike and ii) pulse-feeding mode. In the spike approach, 10 mmol of VA (10 mM final concentration) were added all at once 6 h after the inoculum of the strain *E. coli* MG1655 RARE pCFD: LigV-VanAB pETD:AroY-C12O; in the pulse-feeding method, VA was added at a rate of 1 mmol/h from 6 h after the growth started. In the spike approach, VA was almost completely converted into ccMA in 30 h and vanillic acid accumulation was observed from 8 to 24 h (Fig. 3A). Using the pulse-feed approach, the almost complete conversion of 10 mM VA was reached after 16 h, a time frame significantly lower compared to the spike approach (Fig. 3B). Accordingly, the maximum specific productivity during the pulse-feeding mode (0.077 g/L×h × g_{cdw}) was ≈50 % higher than in the spike approach (0.052 g/L×h × g_{cdw}); therefore, the pulse-feed mode was selected for the next bioconversions.

Subsequently, two different bioconversions were set up, both at 40 mM VA final concentration: i) 2 mmol/h VA pulse-feeding for 20 h, to verify whether the engineered strain was able to maintain the same conversion yield at a higher VA addition rate, and ii) 1 mmol/h VA pulse-feeding for 40 h, to test whether the engineered strain maintained its catalytic prowess at a higher VA level when added over a longer time lapse. As shown in Fig. 3C, an accumulation of vanillic acid (≈25 mM at 30 h) in the 2 mmol/h pulse-feeding cultivation was observed, showing that the engineered strain was not able to fully convert VA into ccMA at this feeding rate. Notably, the cells' growth seems impaired by the higher VA feeding rate: the observed saturation density was only ≈3.4 OD/mL (Fig. 3D) vs. a 5.0 – 6.0 OD/mL value reached in the previous cultivations (see supplementary materials). Accordingly, the low biomass concentration in the bioreactor could be responsible for the accumulation of vanillic acid and the low ccMA production yield (Fig. 3C).

Interestingly, the cultivation at 1 mmol/h VA pulse-feeding addition with a duration of 40 h reached a culture saturation density ≈5.0 OD/mL, comparable to the biomass level obtained during the growth analysis (see supplementary materials), and the lactose and glycerol were completely depleted after 24 h and 42 h, respectively (Fig. 3F). Under these conditions, the engineered strain produced ≈36 mM (≈5.2 g/L) ccMA from 40 mM VA over 48 h of incubation (Fig. 3E), thus reaching a ≈90 % VA bioconversion yield. Notably, all the carbon sources were completely depleted during the cultivation (Fig. 3F), demonstrating that the engineered strain hold metabolically active over the 48 h, and that the conversion of VA into ccMA continued even after the lactose was consumed. The conversion of 40 mmol VA into ccMA using 1 mmol/h pulse-feeding approach was thus carried out in triplicate: an overall 91.70 ± 0.06 % yield of VA, with a final ccMA titer of 36.7 ± 2.5 mM was achieved after 48 h, with a similar metabolic profile (see supplementary materials).

The specific activity of each of the four enzymes in the ccMA synthetic pathway in resting cells correspond to 1.08, 8.17, 0.47 and 20.0 nmol/min x mg_{cell} for LigV, VanAB, AroY and C12O, respectively: apparently, the decarboxylation step by AroY should be the rate-limiting step. Anyway, since PCA never accumulated during bioconversion, while vanillic acid did under spike (Fig. 3A) or high rate pulse-feed addition (Fig. 3C), VA dehydrogenation by LigV seems the rate-limiting step under bioconversion conditions. The addition of VA using a pulse-feed strategy (1 mmol/h – 0.153 g/L×h) represents the best strategy to reduce the inhibition of VanA activity from vanillic acid accumulation (Chen et al., 2021). Under pulse feeding conditions, the productivity (expressed as g ccMA/L×h × g cells) is in all cases ≥ 2-fold higher than using a single VA addition (0.04–0.05 vs. 0.02, respectively). The optimized growth medium composition and the substrate's addition strategy allowed the engineered strain to produce 5.2 ± 0.36 g/L of ccMA in 48 h, corresponding to 0.86 $g_{ccMA}/g_{vanillin}$.

3.3. Cis,cis-muconic acid purification

Under the optimized conditions (see above) the supernatant was separated from the biomass through centrifugation and ccMA was purified: a total of 2.58 ± 0.07 g ccMA per liter of supernatant was obtained, corresponding to a recovery yield of 49.5 ± 0.1 %, with a > 95 % purity of ccMA crystals, as evaluated by HPLC analysis (data not shown). The overall purity is crucial for the rate and extent of polymerization (see below), as well as to meet the compositional requirements for renewable chemical and polymer applications (Hiemenz and Lodge, 2007). The absence of organic contaminants has been evaluated by NMR analysis: the ccMA spectrum was comparable to the commercial one (data not shown). Noteworthy, the ccMA crystals showed a purity comparable to the one reported by (Wang et al., 2022) and to the commercial ccMA from chemical origin (i.e. 97.7 %) (Vardon et al., 2016), but with a lower recovery yield. In order to increase the recovery yield, the used activated charcoal was resuspended in water and the purification protocol was restarted from the step involving the incubation at 37 °C for 1 h in agitation (Wang et al., 2022): anyway, no further ccMA was recovered. The lower overall recovery yield could be related to difference in the ccMA concentration in the supernatants, 5.2 g/L (this work) and 20.55 g/L in (Wang et al., 2022), to ccMA losses due to

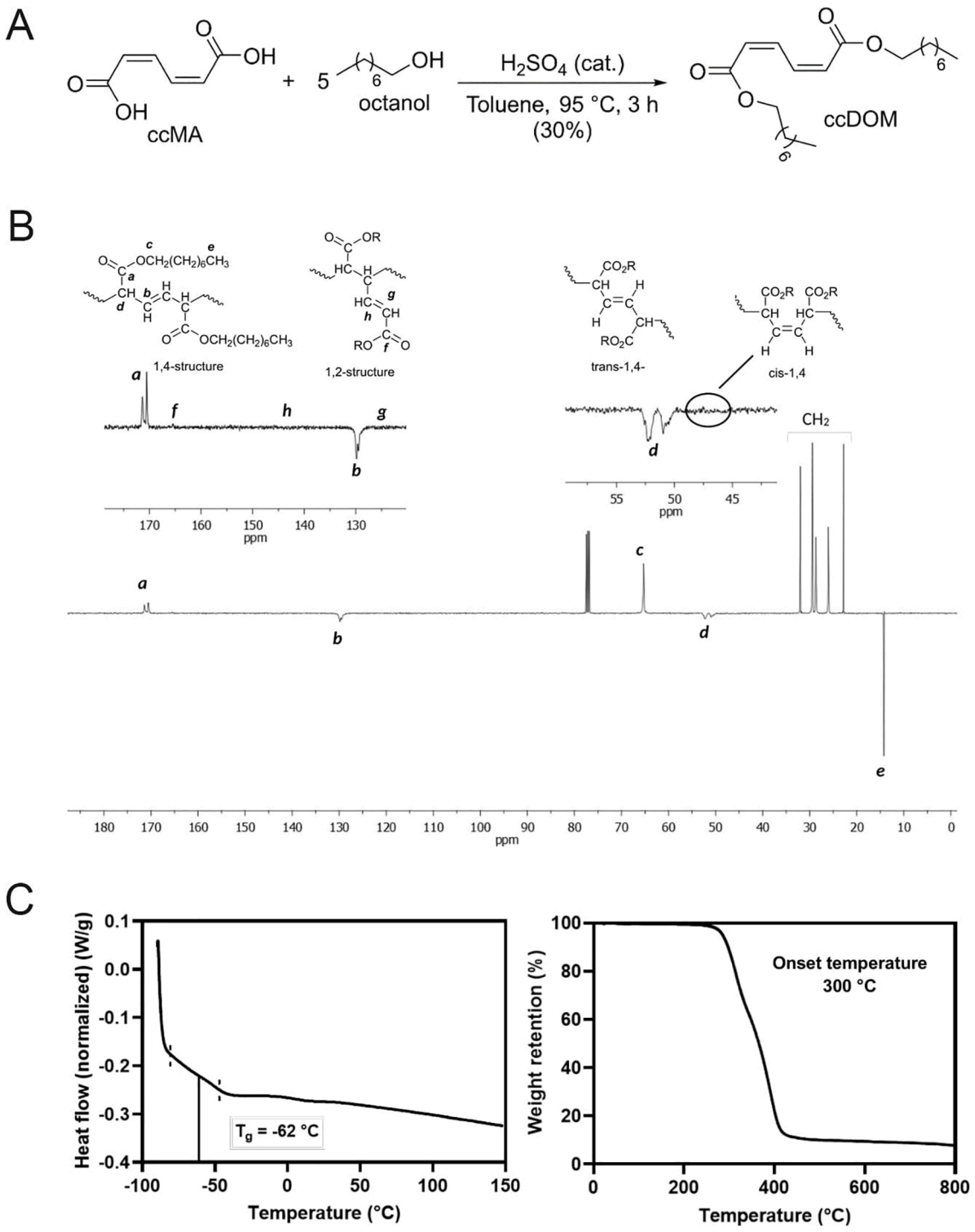

Fig. 4. A) Synthesis of *cis,cis*-dioctyl muconate (ccDOM). B) ^{13}C-{^{1}H} NMR spectrum ($CDCl_3$, 100 MHz, 298 K) of high stereoregular (1,4-*trans*)-PDOM. C) DSC (left) and TGA (right) traces for PDOM produced in this work.

activated charcoal interactions and to the minimal solubility of protonated ccMA in water (≈ 1 g/L) that does not allow the separation of the remaining ccMA by crystallization. Accordingly, the cultivation medium was 4-fold concentrated through lyophilization, obtaining a solution with a ccMA concentration resembling the one reported in (Wang et al., 2022). The resulting solution was processed following the same purification protocol as before, reaching ≈68 % of ccMA recovery yield (3.5 g/L fermentation broth) consistent with the figure reported in literature (Wang et al., 2022).

At the industrial level, recovery techniques are crucial in terms of efficiency and profitability. A number of separation techniques have been used, including membrane separation, precipitation, absorption, reverse osmosis; for a recent review see (Blaga et al., 2023). The reactive extraction approach using a combination of extractants and solvents has recently drawn great attention as a viable and efficient way to recover ccMA from the broth with a yield up to 98.7 % (Blaga et al., 2023). Recently, the biological production of ccMA was performed in a 10-L bioreactor using an engineered strain of *P. putida* KT2440 and purified following a procedure similar to the one we used to be then catalytically converted to adipic acid: residual amino acids and proteins were

Table 2
Free radical polymerization of muconic acid diesters.

Entry	Monomer	T_{exp} (°C)	Time (h)	Conversion (%)[a]	Monomer/initiator ratio	M_n (kDa)[b]	$Đ$[b]	T_g (°C)[c]
1	ccDOM	130	22	64	50	n.d.	n.d	n.d.
2		110	48	80	100	4.2	2.0	−62
3[d]	ttDEM	120	48	78	4000	123.0	1.7	−37

Reaction conditions: anisole, [monomer] = 2 M, initiator = di-*tert*-butyl peroxide (DTBPO). [a]Determined by ^{1}H NMR spectroscopy on the crude reaction mixture. [b]Determined by GPC analysis in THF against PS standards. [c]Determined by DSC analysis (second heating run). [d]Data reported in (Quintens et al., 2019). n.d. = not determined.

removed by microfiltration, followed by color removal with activated charcoal, crystallization by pH/temperature shift, and final dissolution in ethanol to remove insoluble salts (Vardon et al., 2016). Interestingly, a minor fraction of ccMA (2.3 %) was lost during protein separation, a negligible loss was observed in the active charcoal cleanup and, after crystallization (13.6 % loss) and ethanol purification (3.4 % loss), ccMA was recovered from the cell-free culture media with a 81.4 % final yield and 99.8 % purity.

The proposed process could be further optimized by increasing the biomass concentration in the bioreactor, which could lead to a higher achievable ccMA titer allowing for a more effective purification step and making the process industrially viable and better comparable with alternative bacterial strains (Becker et al., 2018; Johnson et al., 2016). Concerning the implementation of the bioconversion process at large scale, the main aspects to be considered are mass-transfer, enzymatic activity, ease of operation and reusability of the biocatalyst: immobilization is often crucial for enhancing the operational performance of an enzyme. In this view, the packed-bed reactor could represent a promising configuration for conducting enzymatic conversions with immobilized biocatalysts, allowing higher volumetric productivity and the possibility to operate continuously, thus facilitating the downstream processing. Similarly, the adaptive laboratory evolution technique could be employed to select productive industrial strains.

3.4. High regio- and stereoregular cis,cis-muconic acid-based polymers with tailored physico-chemical properties

The valorization of isomers of MA wanders from the synthesis of added-value chemicals, such as adipic or terefthalic acid, to novel polymers. Polymer from MA has been first synthesized by free radical polymerization (FRP) in 1977 along with its diethyl ester (Bando et al., 1977). However, the corresponding diesters are preferred in radical polymerization due to both their enhanced solubility and absence of carboxy groups that can interfere with the radical propagation (Quintens et al., 2019). MA is a conjugated diene similar to butadiene, a monomer that produces polybutadiene, the first and one of the most used synthetic rubbers, characterized by very low glass transition temperature (T_g). Despite the conjugated diene structure, diesters deriving from MA afford polymers with a variety of T_g values depending on the nature of the ester groups. According to the literature, T_g of polymuconates significantly decreases upon increasing the length of ester side chain of the muconates: the T_g of poly(diethyl muconate) (PDEM) is around 7 °C, while that of poly(dibutyl muconate) drops to −37 °C. Even materials derived from branched esters, i.e. poly(diethyl hexyl muconate), exhibit low T_g values (−60 °C). We aimed at synthesizing a polymer exhibiting T_g values comparable to that of rubbers, since MA diester can provide unsaturated carbon–carbon bond in the polymer structure similarly to poly(butadiene).

For the synthesis of the diester from ccMA, octanol was selected both because of its long-chain, useful to the targeted properties of the final polymer, and for the bioavailability, since it can be produced from engineered bacteria such as *Synechocystis* sp. PCC 6803 (Yunus et al., 2021) and *E. coli* (Lozada et al., 2020). ccMA was functionalized by Fisher esterification to obtain *cis,cis*-dioctyl muconate (ccDOM). Optimization of the reaction conditions (see supplementary materials) allowed for the isolation of crystalline ccDOM within 3 h under mild conditions (Fig. 4A), guaranteeing a greener approach compared to reported procedures mainly employing thionyl chloride ($SOCl_2$). Furthermore, a commercial ccMA was employed for the synthesis of ccDOM using the same procedure described above: final mixture composition was comparable to that produced by ccMA generated by the bioconversion process (see supplementary materials). The product was characterized by NMR- and IR- spectroscopy analyses as well as via differential scanning calorimetry (see supplementary materials). Aiming at reducing the environmental impact of the polymerization of ccDOM, test of polymerization of ccDOM were carried out in anisole, a green and recyclable solvent. As the FRP of conjugated dienes requires high temperatures to achieve good conversions, di-*tert*-butyl peroxide (DTBPO), displaying a 10 h half-life at 123 °C, was selected as the radical initiator. The experimental conditions and monomer conversion are reported in Table 2. Noteworthy, 80 % of monomer conversion was achieved within 48 h at 110 °C upon employing a ccDOM/DTBPO ratio of 100 (Table 2, entry 2). This was in agreement with what reported for the polymerization of DEM (78 %) derived from the commercially available *trans, trans* isomer of muconic acid (Quintens et al., 2019). The higher molecular mass observed in this condition could be related to the higher monomer/initiator ratio used (4000:1, Table 2, entry 3). The spectroscopic analysis of the polymer is reported in supplementary materials.

Similarly to other conjugated diene monomers (i.e. butadiene), the polymerization of muconic esters can in principle propagate through 1,2- and 1,4-radical addition. Furthermore, the 1,4-addition can result in *cis* and *trans* conformations (see supplementary materials). The microstructure of the polymer greatly influences the physico-chemical properties of the material, hence different polymerization conditions are generally employed to produce polymers with the desired regio- and stereoregularity. Specifically, FRP of butadiene carried out at 100 °C results in polymers with about 28 % of 1,4-*cis*, 51 % of 1,4-*trans* and 21 % of 1,2 addition. The ratio among the different additions can be somewhat modulated acting on the temperature of polymerization. Opposite to butadiene, muconate diesters generally produce mainly 1,4-*trans* polymuconates with low amount of 1,2 addition (about 2 %) and 1,4-*cis* (11–13 %), depending on the experimental conditions (Matsumoto et al., 1996). Noteworthy, the ^{13}C-{^{1}H} NMR spectrum of the PDOM obtained at 110 °C (Table 2, entry 2) displayed resonances accountable only to *trans*-1,4 structures, and *cis*-1,4- and 1,2-structures were not detected (Fig. 4B).

Overall, the results indicate that the ccMA obtained from lignin through engineered bacteria is suitable for polymer applications, as building block for the synthesis of new materials with yields comparable to those obtained from commercially available muconates. The overall optimized workflow for the production of PDOM from VA is reported in Fig. 1B.

One of the most important technological parameters for polymers is the glass transition temperature, which was determined for PDOM obtained at 110 °C (Table 2, entry 2) by DSC measurement as shown in Fig. 4C, left. The thermogram reported is referred to the second heating cycle, thus after removal of the thermal history of the polymer: the T_g value is around – 62 °C. This is in accordance with what predicted by

Table 3
Comparison between the green metrics of bioconversion processes using resting cells, cultivation with growing cells alone, and the cultivation process plus the downstream ccMA purification step.

	Stoichiometric Factor (SF) (Andraos, 2005)	Carbon Efficiency (CE) (Constable et al., 2001)	Atom Efficiency (AE) (Trost, 1991)	Actual AE (AAE) (Trost, 1991)	E-value (Sheldon, 1997)	Process Mass Intensity (PMI) (Curzons et al., 2001)
Resting cells	1.0	67.5	93.4	93.4	30.2	1417.1
Growing cells	1.0	67.5	93.4	84.1	0.4	195.2
+ ccMA purification				57.2	28.8	315.0

increasing the length of the ester side chain of muconates. As reported by (Quintens et al., 2019), the trend of T_g for different poly-muconates is similar to what observed for the corresponding acrylate polymers. This was also confirmed for our sample, since the T_g of poly(n-octyl acrylate) and of poly(2-ethyl-hexyl acrylate) are ≈ −70 °C and −64 °C, respectively (Fleischhaker et al., 2014; Li et al., 2021). TGA measurement (Fig. 4C, right) was carried out under nitrogen atmosphere to evaluate the thermal stability of PDOM (Table 2, entry 2). The decomposition started at 300 °C and the polymer was fully degraded at 430 °C.

3.5. Green metrics

As shown in Table 3, green metrics have been calculated for the bioconversion of VA into ccMA using both the resting cells strategy described in our previous work (Molinari et al., 2023) and the growing cells process (plus the downstream ccMA purification step) optimized in the present work. For a better comparison of two different strategies of biocatalysis, metrics have been evaluated by calculating the amount of biomass, substrate and solutions needed to produce the ccMA obtained by the fermentative process (i.e. 5.2 g/L). The AE, CE and SF are the same for all bioconversion processes due to using the same biocatalytic pathway, since these parameters evaluate the amount of substrate mass retained in the product (Andraos, 2005; Constable et al., 2001). The bioconversion using resting cells showed a higher AAE value compared to the process performed by fermentation due to the higher conversion rate (this parameter is calculated by multiplying AE by product's relative yield). The E-value is the ratio of the amount of waste produced to the amount of product obtained (Sheldon, 1997) and the PMI is the ratio of the amount of materials used for the process to the amount of product obtained (Curzons et al., 2001). The approach using growing cells is clearly more sustainable than the resting cells one with lower PMI and E-value even when the purification step is taken into consideration, see supplementary materials. Comparing the E-factor of our processes with the ones designated by (Sheldon, 1997), the process based on growing cells alone has an E-value suitable for the production of bulk chemicals (<1–5 $kg_{product}/kg_{waste}$) while when the purification step is considered the E-value arose to a figure acceptable for the production of fine chemicals (5–50 $kg_{product}/kg_{waste}$).

The values reported in Table 3 highlight that the approach based on growing cells is more sustainable compared to the bioconversion with resting cells, despite the lower AAE, even when combined with the product purification step. This is due to the lower number of steps, thus removing the use of buffer salts and additional water, and the lower amount of biocatalyst for the fermentative process (2 g cdw vs. 36 g cdw). The ccMA purification step has not been considered for the resting cells process because of the lower ccMA titer (1.42 g/L) that does not allow an efficient crystallization.

A comparison of the biocatalytic parameters for bioconversions performed with resting cells and the fermentative process is shown in supplementary materials; the latter process was evaluated also considering the biocatalyst preparation step (requiring a total of 26 h) and the 2 h bioconversion reaction. The process with growing cells reached a 4-fold higher ccMA production compared to resting cells: a figure of 5.2 and 1.42 g/L was achieved, respectively. ccMA volumetric production is even most notable when normalized on the amount of cells utilized in the bioconversion (2 and 10 g_{cdw}/L in the growing and resting cells approach, respectively): it is ≈17-fold higher in the fermentation (2.6 vs. 0.14 g/L×g_{cdw}). On the other hand, the resting cells approach showed better volumetric productivity (0.7 g/L×h) and specific productivity (0.07 g/L×h g_{cdw}) in comparison to the growing cells process (0.11 g/L×h and 0.05 g/L×h g_{cdw}, respectively). Nonetheless, when the preparation step of the resting cells process is taken into consideration, the average volumetric productivity is ≈2-fold lower than with resting cells (0.11 vs. 0.05 g/L×h). This difference increased to ≈10-fold (0.05 vs. 0.005 g/L×h g_{cdw}) when normalized on the amount of cells utilized. Moreover, the maximum specific productivity of the growing cells (0.12 g/L×h×g_{cdw}) is ≈60 % higher than the specific productivity of the resting cells (0.07 g/L×h×g_{cdw}), and 24-fold higher when the biocatalyst preparation is considered (0.005 g/L×h×g_{cdw}).

4. Conclusions

To the best of our knowledge, this is the first report of a biocatalytic process producing ccMA from VA using an engineered *E. coli* strain grown in a bioreactor. Despite the improvements of using growing cells over the resting cells approach, this is a pilot-study on the possible production of plastic monomer precursors from lignin-derived feedstocks for polymer applications. The development of an innovative platform will represent a novel paradigm approach contributing to the development of more sustainable and efficient processes for the valorization of renewable biomasses, with a broader implication for the transition to a circular bioeconomy.

CRediT authorship contribution statement

Filippo Molinari: Writing – original draft, Visualization, Methodology. **Andrea Salini:** Visualization, Methodology. **Aniello Vittore:** Visualization, Methodology. **Orlando Santoro:** Visualization, Methodology. **Lorella Izzo:** Writing – original draft, Supervision, Project administration, Funding acquisition, Conceptualization. **Salvatore Fusco:** Writing – review & editing, Supervision, Funding acquisition, Conceptualization. **Loredano Pollegioni:** Writing – original draft, Supervision, Project administration, Funding acquisition, Conceptualization. **Elena Rosini:** Writing – original draft, Supervision, Project administration, Funding acquisition, Conceptualization.

Declaration of competing interest

The authors declare that they have no known competing financial interests or personal relationships that could have appeared to influence the work reported in this paper.

Data availability

Data will be made available on request.

Acknowledgments

LP and FM thank the support of CIRCC-Consorzio Interuniversitario per le Reattività Chimiche e la Catalisi. FM is a student of the PhD course

"Life Sciences and Biotechnology", University of Insubria. AV is a student of the PhD course "Chemical and Environmental Sciences" University of Insubria, supported by ESF (European Social Fund) - REACT-EU Programme (DM 1061/2021). OS thanks the support by ESF (European Social Fund) - REACT-EU Programme (DM 1062/2021). LI thanks the support by MUR (Italian Ministry of University and Research)- FAR 2023. SF thanks the support by MUR (Italian Ministry of University and Research) - grant number "CUP B31I18000230006". This publication is part of the project NODES which has received funding from the MUR – M4C2 1.5 of PNRR funded by the European Union - NextGenerationEU (Grant agreement no. ECS00000036).

Appendix A. Supplementary data

Supplementary data to this article can be found online at https://doi.org/10.1016/j.biortech.2024.131190.

References

Andraos, J., 2005. Unification of reaction metrics for green chemistry: applications to reaction analysis. Org. Process Res. Dev. 9, 149–163. https://doi.org/10.1021/op049803n.

Bando, Y., Dodou, T., Minoura, Y., 1977. Radical polymerization of muconic acid and ethyl muconate. Polym. Sci. Polym. Chem. Ed. 15, 1917–1926.

Becker, J., Kuhl, M., Kohlstedt, M., Starck, S., Wittmann, C., 2018. Metabolic engineering of Corynebacterium glutamicum for the production of cis, cis-muconic acid from lignin. Microb, Cell. 17, 115. https://doi.org/10.1186/s12934-018-0963-2.

Becker, J., Wittmann, C., 2019. A field of dreams: Lignin valorization into chemicals, materials, fuels, and health-care products. Biotechnol. Adv. 37 https://doi.org/10.1016/j.biotechadv.2019.02.016.

Blaga, A.C., Gal, D.G., Tucaliuc, A., 2023. Recent advances in muconic acid extraction process. Appl. Sci. 13 https://doi.org/10.3390/app132111691.

Blommel, P.G., Becker, K.J., Duvnjak, P., Fox, B.G., 2007. Enhanced bacterial protein expression during auto-induction obtained by alteration of lac repressor dosage and medium composition. Biotechnol. Prog. 23, 585–598. https://doi.org/10.1021/bp070011x.

Cardoso, V.M., Campani, G., Santos, M.P., Silva, G.G., Pires, M.C., Gonçalves, V.M., Giordano, R.D.C., Sargo, C.R., Horta, A.C.L., Zangirolami, T.C., 2020. Cost analysis based on bioreactor cultivation conditions: Production of a soluble recombinant protein using Escherichia coli BL21 (DE3). Biotechnol. Reports 26. https://doi.org/10.1016/j.btre.2020.e00441.

Chen, Y., Fu, B., Xiao, G., Ko, L.-Y., Kao, T.-Y., Fan, C., Yuan, J., 2021. Bioconversion of lignin-derived feedstocks to muconic acid by whole-cell biocatalysis. ACS Food Sci. Technol. 1, 382–387. https://doi.org/10.1021/acsfoodscitech.1c00023.

Choi, S., Lee, H.N., Park, E., Lee, S.J., Kim, E.S., 2020. Recent advances in microbial production of cis, cis-muconic acid. Biomolecules 10, 1–14. https://doi.org/10.3390/biom10091238.

Choi, S.S., Seo, S.Y., Park, S.O., Lee, H.N., Song, J.S., Kim, J.Y., Park, J.H., Kim, S., Lee, S. J., Chun, G.T., Kim, E.S., 2019. Cell factory design and culture process optimization for dehydroshikimate biosynthesis in Escherichia coli. Front. Bioeng. Biotechnol. 7 https://doi.org/10.3389/fbioe.2019.00241.

Constable, D.J.C., Curzons, A.D., Freitas dos Santos, L.M., Geen, G.R., Hannah, R.E., Hayler, J.D., Kitteringham, J., McGuire, M.A., Richardson, J.E., Smith, P., Webb, R. L., Yu, M., 2001. Green chemistry measures for process research and development. Green Chem. 3, 7–9. https://doi.org/10.1039/b007875l.

Curzons, A.D., Constable, D.J.C., Mortimer, D.N., Cunningham, V.L., 2001. So you think your process is green, how do you know? - Using principles of sustainability to determine what is green - A corporate perspective. Green Chem. 3, 1–6. https://doi.org/10.1039/b007871i.

Dvorak, P., Chrast, L., Nikel, P.I., Fedr, R., Soucek, K., Sedlackova, M., Chaloupkova, R., de Lorenzo, V., Prokop, Z., Damborsky, J., 2015. Exacerbation of substrate toxicity by IPTG in Escherichia coli BL21(DE3) carrying a synthetic metabolic pathway. Microb. Cell Fact. 14, 201. https://doi.org/10.1186/s12934-015-0393-3.

Fitzgerald, D.J., Stratford, M., Gasson, M.J., Ueckert, J., Bos, A., Narbad, A., 2004. Mode of antimicrobial of vanillin against Escherichia coli, Lactobacillus plantarum and Listeria innocua. J. Appl. Microbiol. 97, 104–113. https://doi.org/10.1111/j.1365-2672.2004.02275.x.

Fleischhaker, F., Haehnel, A.P., Misske, A.M., Blanchot, M., Haremza, S., Barner-Kowollik, C., 2014. Glass-transition-, melting-, and decomposition temperatures of tailored polyacrylates and polymethacrylates: General trends and structure-property relationships. Macromol. Chem. Phys. 215, 1192–1200. https://doi.org/10.1002/MACP.201400062.

Gaglione, R., Pane, K., Dell'Olmo, E., Cafaro, V., Pizzo, E., Olivieri, G., Notomista, E., Arciello, A., 2019. Cost-effective production of recombinant peptides in Escherichia coli. N. Biotechnol. 51, 39–48. https://doi.org/10.1016/j.nbt.2019.02.004.

Hiemenz, P.C., Lodge, T., 2007. Polymer chemistry (2nd edition) 587.

Johnson, C.W., Salvachúa, D., Khanna, P., Smith, H., Peterson, D.J., Beckham, G.T., 2016. Enhancing muconic acid production from glucose and lignin-derived aromatic compounds via increased protocatechuate decarboxylase activity. Metab. Eng. Commun. 3, 111–119. https://doi.org/10.1016/j.meteno.2016.04.002.

Kohlstedt, M., Starck, S., Barton, N., Stolzenberger, J., Selzer, M., Mehlmann, K., Schneider, R., Pleissner, D., Rinkel, J., Dickschat, J.S., Venus, J., van Duuren, B.J.H., J., Wittmann, C.,, 2018. From lignin to nylon: Cascaded chemical and biochemical conversion using metabolically engineered Pseudomonas putida. Metab. Eng. 47, 279–293. https://doi.org/10.1016/j.ymben.2018.03.003.

Kunjapur, A.M., Tarasova, Y., Prather, K.L.J., 2014. Synthesis and Accumulation of Aromatic Aldehydes in an Engineered Strain of Escherichia coli. J. Am. Chem. Soc. 136, 11644–11654. https://doi.org/10.1021/ja506664a.

Li, T., Li, H., Wang, H., Lu, W., Osa, M., Wang, Y., Mays, J., Hong, K., 2021. Chain flexibility and glass transition temperatures of poly(n-alkyl (meth) acrylate)s: Implications of tacticity and chain dynamics ☆. Polymer (guildf). 213, 123207 https://doi.org/10.1016/j.polymer.2020.123207.

Long, J., Zhang, Q., Wang, T., Zhang, X., Xu, Y., Ma, L., 2014. An efficient and economical process for lignin depolymerization in biomass-derived solvent tetrahydrofuran. Bioresour. Technol. 154, 10–17. https://doi.org/10.1016/j.biortech.2013.12.020.

Lozada, N.J.H., Simmons, T.R., Xu, K., Jindra, M.A., Pfleger, B.F., 2020. Production of 1-octanol in Escherichia coli by a high flux thioesterase route. Metab. Eng. 61, 1096–7176. https://doi.org/10.1016/j.ymben.2020.07.004.

Matsumoto, A., Matsumura, T., Aoki, S., 1996. Stereospecific polymerization of dialkyl muconates through free radical polymerization: Isotropic polymerization and topochemical polymerization. Macromolecules 29, 423–432. https://doi.org/10.1021/MA950996B.

Matthews, B.W., 2005. The structure of E. coli β-galactosidase. C. r. Biol. 328, 549–556. https://doi.org/10.1016/J.CRVI.2005.03.006.

Mayer, S., Junne, S., Ukkonen, K., Glazyrina, J., Glauche, F., Neubauer, P., Vasala, A., 2014. Lactose autoinduction with enzymatic glucose release: Characterization of the cultivation system in bioreactor. Protein Expr. Purif. 94, 67–72. https://doi.org/10.1016/J.PEP.2013.10.024.

Molinari, F., Pollegioni, L., Rosini, E., 2023. Whole-Cell Bioconversion of Renewable Biomasses-Related Aromatics to cis, cis-Muconic Acid. ACS Sustain. Chem. Eng. 11, 2476–2485. https://doi.org/10.1021/acssuschemeng.2c06534.

Phillips, R., Milo, R., 2009. A feeling for the numbers in biology. Proc. Natl. Acad. Sci. u. s. a. 106, 21465–21471. https://doi.org/10.1073/pnas.0907732106.

Pollegioni, L., Tonin, F., Rosini, E., 2015. Lignin-degrading enzymes. FEBS J 282, 1190–1213. https://doi.org/10.1111/febs.13224.

Quintens, G., Vrijsen, J.H., Adriaensens, P., Vanderzande, D., Junkers, T., 2019. Muconic acid esters as bio-based acrylate mimics. Polym. Chem. 10, 5555. https://doi.org/10.1039/c9py01313j.

Rosini, E., Molinari, F., Miani, D., Pollegioni, L., 2023. Lignin Valorization: Production of High Value-Added Compounds by Engineered Microorganisms. Catalysts 13. https://doi.org/10.3390/catal13030555.

Sezonov, G., Joseleau-Petit, D., D'Ari, R., 2007. Escherichia coli physiology in Luria-Bertani broth. J. Bacteriol. 189, 8746–8749. https://doi.org/10.1128/JB.01368-07.

Sheldon, R.A., 1997. Catalysis: The key to waste minimization. J. Chem. Technol. Biotechnol. 68, 381–388. https://doi.org/10.1002/(SICI)1097-4660(199704)68:4<381::AID-JCTB620>3.0.CO;2-3.

Studier, F.W., 2005. Protein production by auto-induction in high density shaking cultures. Protein Expr. Purif. 41, 207–234. https://doi.org/10.1016/j.pep.2005.01.016.

Trost, B.M., 1991. The Atom Economy - A Search for Synthetic Efficiency. Science 80-.). 254, 1471–1477.

Vardon, D.R., Rorrer, N.A., Salvachúa, D., Settle, A.E., Christopher, W.J., Menart, M.J., Cleveland, N.S., Ciesielski, P.N., Steirer, K.X., Dorgan, J.R., Beckham, G.T., 2016. *cis*, *cis*-Muconic acid: separation and catalysis to bio-adipic acid for nylon-6,6 polymerization. Green Chemistry 18, 3397–3413. https://doi.org/10.1039/C5GC02844Bhw45hw4jw4jw46j.

Vignali, E., Pollegioni, L., Nardo, G.D., Valetti, F., Gazzola, S., Gilardi, G., Rosini, E., 2021. Multi-Enzymatic Cascade Reactions for the Synthesis of cis, cis-Muconic Acid. Adv. Synth. Catal. 364, 114–123. https://doi.org/10.1002/adsc.202100849.

Vignali, E., Gigli, M., Cailotto, S., Pollegioni, L., Rosini, E., 2022. The Laccase-Lig Multienzymatic Multistep System in Lignin Valorization. ChemSusChem 15, e202201147.

Wang, G., Tavares, A., Schmitz, S., França, L., Almeida, H., Cavalheiro, J., Carolas, A., Øzmerih, S., Blank, L.M., Ferreira, B.S., Borodina, I., 2022. An integrated yeast-based process for cis, cis-muconic acid production. Biotechnol. Bioeng. 119, 376–387. https://doi.org/10.1002/bit.27992.

Yunus, I.S., Wang, Z., Sattayawat, P., Muller, J., Zemichael, F.W., Hellgardt, K., Jones, P. R., 2021. Improved Bioproduction of 1-Octanol Using Engineered Synechocystis sp. PCC 6803. ACS Synth. Biol. 10, 1417–1428. https://doi.org/10.1021/acssynbio.1c00029.

Zhang, H., Li, Z., Pereira, B., Stephanopoulos, G., 2015. Engineering E. coli-E. coli cocultures for production of muconic acid from glycerol. Microb. Cell Fact. 14, 1–10. https://doi.org/10.1186/s12934-015-0319-0.

Zwietering, M.H., Jongenburger, I., Rombouts, F.M., Van't Riet, K.,, 1990. Modeling of the Bacterial Growth Curve. Appl. Environ. Microbiol. 56, 1875. https://doi.org/10.1128/AEM.56.6.1875-1881.1990.